Supplementary Information (SI) for ChemComm.

Electronic Supplementary Information for

Pushing the Limit of Triplet-Triplet Annihilation Photon Upconversion Towards the UVC Range

Till J. B. Zähringer,[a] Corinna Heusel,[b] Matthias Schmitz,[a] Frank Glorius[b] and Christoph Kerzig*[a]

[a] Department of Chemistry, Johannes Gutenberg University Mainz, Duesbergweg 10–14, 55128, Mainz, Germany.
[b] Organisch-Chemisches Institut, University of Münster, Corrensstraße 36, 48149, Münster, Germany.

Email: ckerzig@uni-mainz.de

Contents

General experimental details and methods

1.1 Materials

Unless specifically mentioned, all chemicals used for synthesis, irradiation experiments, or optical spectroscopy were commercially obtained and used as received. Tetrahydrofuran, 99.7%, VWR; (triisopropylsilyl)acetylene, 97%, Alfa Aesar; bis(triphenylphosphine)palladium(II) dichloride, 98%, Acros Organics; copper(I) iodide, 99.9%, Alfa Aesar; triphenylphosphine, 99%, Sigma-Aldrich; diisopropylamine, 99.9%, Sigma-Aldrich; bromobenzene, Sigma-Aldrich, 99%; 4-tert-butylbromobenzene, 97%, Avocado; cyclohexane, >99.5%, VWR; benzene, Sigma-Aldrich, 99.9%; acetonitrile, 99.7%, VWR, sodium sulfate, 99%, Acros Organics; $CDCl_3$, 99.8%, Deutero.

Argon from Nippon Gases (5.0) was used for removing dissolved oxygen before all experiments related to optical spectroscopy.

fac-[Ir(CF_3-pmb)$_3$][1] was synthesized according to a literature procedure by Glorius and Guldi.[2]

1.2 Steady-state measurements

Steady-state emission measurements at room temperature were performed using a Perkin Elmer FL-6500 spectrometer. Absorption spectra were recorded with a Perkin Elmer LAMBDA 365 UV-Vis spectrophotometer. All spectra were recorded at room temperature (295 ± 3 K) using quartz glass cuvettes. Emission spectra were corrected regarding the wavelength-dependent sensitivity of the instrument. Low concentrations were used to eliminate filter effects.

1.3 Determination of fluorescence quantum yields

The fluorescence quantum yield of TIPS-Bz was determined in relation to a reference system "ref" (naphthalene in cyclohexane, $\Phi = 0.23$)[3] by the comparison of their respective fluorescence emission spectra. In equation (1) Φ_{Fl} depicts the quantum yield, I the fluorescence intensity integrated over the wavenumber, A the absorption at the irradiation wavelength, and n the refractive index of the solvent of the corresponding system taken from literature.[3] The fluorescence quantum yield for TIPS-Bz was measured at four different excitation wavelengths (250, 255, 260 and 265 nm) and averaged over all results. The systems used to determine the fluorescence quantum yields were prepared with an optical density below 0.1 at the irradiation wavelengths to circumvent filter effects.

$$\phi_{\mathrm{Fl}} = \phi_{\mathrm{Fl,ref}} \cdot \frac{I}{I_{\mathrm{ref}}} \cdot \frac{A_{\mathrm{ref}}}{A} \cdot \frac{n^2}{n_{\mathrm{ref}}^2} \tag{1}$$

1.4 Laser flash photolysis

The LP980KS system from Edinburgh Instruments, equipped with a Quantel Nd:YAG laser (Q-smart 450), was used for transient absorption and time-resolved emission spectroscopy. The laser's frequency-tripled output at 355 nm served as the excitation source, delivering pulses of ~ 5 ns duration at a repetition rate of 10 Hz. If not stated otherwise, the pulse energy applied in transient absorption and emission experiments was 20 mJ. Transient absorption spectra were recorded using an Andor iCCD camera, while kinetic traces at selected wavelengths were obtained via a photomultiplier tube. To ensure consistent laser pulse energy across experiments, power measurements were conducted before, during and after each series of experiments using a Gentec-eo pyroelectric detector with an attenuator (QE25LP-S-MB-QED-D0) and the Integra software was used for evaluation. Spectroscopic experiments were performed at 293 K with a temperature-controlled cuvette holder. Unless otherwise noted, transient absorption spectra were integrated over 100 ns. For detection wavelengths exceeding 600 nm, longpass filters (385 nm or 400 nm, Newport) were used to eliminate contributions from second-order signals.

1.5 Fluorescence lifetime measurements

The *mini-τ* setup from Edinburgh Instruments (time-correlated single photon counting (TCSPC) technique) equipped with a pulsed LED (EPLED-300, excitation at ~293 nm, pulse width ~ 1 ns, bandwidth = 10.7 nm) was employed for fluorescence lifetime measurements of TIPS-Bz at 293 K.

1.6 Chromatography

For **TIPS-Bz** standard liquid column chromatography separation silica gel 60 M (0.040-0.063 mm Macherey-Nagel GmbH & Co., Düren, Germany) was used. Thin layer chromatography (TLC) was performed using "DC Kieselgel 60 F254" (Merck KGaA, Darmstadt, Germany) on aluminum and a UV lamp (Benda, NU-4 KL, λ = 254 nm and 365 nm, Wiesloch, Germany) was employed for detection. Reversed-phase column chromatographic purification was carried out for **4tBu-TIPS-Bz** using the Isolera One automated chromatography system, which includes the Isolera™ Dalton detector from Biotage. A SNAP Cartridge KP-C18-HS from Biotage was used as the column material. The resulting R_f values are given relative to the solvent.

1.7 NMR spectroscopy

NMR spectra of **TIPS-Bz** and **4tBu-TIPS-Bz** were recorded with a multinuclear magnetic resonance spectrometer of the type AV II 400 (Bruker, Karlsruhe, Germany) was employed. The chemical shifts are given as δ-values in ppm and they were referenced relative to the residue signal of the non-deuterated solvent.[4] The following abbreviations were used: singlet (s), doublet (d), multiplet (m).

1.8 Mass spectrometry

Low-resolution FD mass spectra for **TIPS-Bz** and **4tBu-TIPS-Bz** were acquired using a Thermo Fisher DFS mass spectrometer equipped with an LIFDI upgrade from Linden ChroMasSpec GmbH, configured for FD mode. Ion source parameters were set as follows: acceleration voltage, +5 kV; counter electrode voltage, -5 kV; reference inlet temperature, 80°C; ion source temperature, 50°C; scan duration: 8 s; interscan delay: 200 ms. CarboTec 10 µm Allround emitter was used, operating at 75 mA. Prior to sample runs, new emitters underwent a preconditioning process involving 2 hours of heating with emitter heating current. Toluene was used as a solvent to deposit the sample onto the emitter. DFS MS scanned from m/z 100 to 1000 at a rate of 8 s/decay.

2. Synthetic procedures

The TIPS-ethynyl-functionalized benzenes were synthesized according to the Sonogashira coupling reaction analogous to the preparation of similar aromatic compounds.[5–7] Exact quantities are listed for each benzene derivative below. The bromobenzene, $Pd(PPh_3)_2Cl_2$, CuI, PPh_3, and dry THF were added to a flame-dried round-bottom flask under argon flow. The flask was equipped with a condenser column. Diisopropylamine was added to the solution under constant stirring. The flask was then heated to 70°C and (triisopropylsilyl)acetylene was added dropwise to the mixture. The mixture was held at 70°C for 12 h under argon atmosphere. The completion of the reaction was tested with TLC. After cooling, the mixture was filtered and the solvent was removed under reduced pressure. The residue was redissolved in chloroform and washed twice with deionized water and twice with brine. The organic layer was dried with Na_2SO_4 and the solvent was removed under reduced pressure. If not stated otherwise, the product was purified via column chromatography (neat cyclohexane). NMR spectra (see below) of all TIPS-ethynyl-benzenes derivatives agree with those reported in the literature.[8]

Triisopropyl(phenylethynyl)silane (TIPS-Bz): **TIPS-Bz** was used from a prior batch, for which the preparation was as follows.[7] 675 mg bromobenzene (4.30 mmol), 18.26 mg $Pd(PPh_3)_2Cl_2$ (0.026 mmol), 13.1 mg CuI (0.069 mmol), 18 mg PPh_3 (0.069 mmol), 28 mL dry THF, 7 mL diisopropylamine and 0.93 mL (triisopropylsilyl)acetylene (4.13 mmol); yield = 354 mg, 1.37 mmol (32%).

A colorless liquid was obtained from column chromatography, which was then distilled under vacuum (10^{-2} mbar) at 80°C.

R_f(cyclohexane) = 0.75

^{1}H NMR (400 MHz, $CDCl_3$): δ [ppm] = 7.29-7.32 (m, 3H), 7.47-7.49 (m, 2H), 1.13 (pseudo-s, 21H).

^{13}C NMR (400 MHz, $CDCl_3$): δ [ppm] = 132.2, 128.4, 128.32, 123.7, 107.2, 90.6, 18.8, 11.5.

MS (FD): m/z [int. I %] = 258.4 [M^+] (100 %); 259.3 (22%); 260.4.4 (5%). Calculated for $C_{17}H_{26}Si$ = 258.2.

NMR spectra are shown in the supporting information document of Ref[7]. Recently recorded NMR and UV/Vis spectra are unchanged compared to those presented in Ref[7].

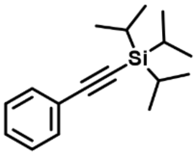

((4-(tert-Butyl)phenyl)ethynyl)triisopropylsilane (4tBu-TIPS-Bz):

1832 mg 4-tert-butylbromobenzene (8.6 mmol), 73.0 mg $Pd(PPh_3)_2Cl_2$ (0.104 mmol), 52.4 mg CuI (0.28 mmol), 72.2 mg PPh_3 (0.28 mmol), 60 mL dry THF, 27 mL diisopropylamine and 3.7 mL (triisopropylsilyl)acetylene (16.92 mmol); yield = 950 mg, 3.02 mmol (32%).

A colorless liquid was obtained after distilliation under vacuum (1.4 10^{-2} mbar) at 200°C. Further purification was achieved by reverse-phase column chromatography: acetonitrile and water were employed as the mobile phase. The crude product was dissolved in DMSO and applied to the column. Chromatographic separation was performed using a gradient of acetonitrile from 10% to 100% over approximately 10 minutes.

We thank Prof. Till Opatz for allowing us to use their equipment for the final purification step.

R_f(water/acetonitrile (1/9)) = 0.80

^{1}H NMR (400 MHz, $CDCl_3$): δ [ppm] = 7.41-7.44 (m, 2H), 7.30-7.34 (m, 2H), 1.32 (s, 9H), 1.13 (s, 21).

^{13}C NMR (400 MHz, $CDCl_3$): δ [ppm] = 151.7, 131.9, 125.3, 120.7, 107.4, 89.8, 34.9, 31.3, 18.9, 11.5.

MS (FD): m/z [int. I %] = 314.4 [M^+] (100 %); 315.4 (24%); 316.4 (5%). Calculated for $C_{21}H_{34}Si$ = 314.2.

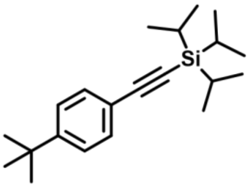

3. DFT calculations

Quantum-chemical calculations were performed with the program Orca 6.0[9] using the functional B3LYP and 6-311+G(d,p) as basis set. After each geometry optimization, vibrational frequencies were calculated. In each case, no imaginary vibration frequencies were obtained, indicating convergence on minimum structures. Geometry optimization of the triplet state was performed starting from the energy-minimized singlet ground state geometry as initial guess. The triplet state energy (adiabatic) was determined by subtracting the energy of the optimized triplet state from the energy of the optimized singlet ground state. This approach has been previously validated as an accurate method for estimating experimental triplet state energies in studies of TIPS-ethynyl-substituted benzenes.[7] To determine electronic excitation energies and oscillator strengths of the lowest 50 transitions, TD-DFT calculations were performed with the previously geometry-optimized structure at the same level of theory. Additional single-point calculations were carried out to obtain the spin densities of the optimized triplet state based on Mulliken population analysis. The structures and spin densities (iso value: 0.005) were displayed using the software Avogadro1.2.0.[10] The color code for the atoms in the ball and stick representation is as follows: carbon (black), hydrogen (white), silicon (petrol blue). In the depiction of spin densities, blue-colored surfaces denote positive spin densities, whereas red-colored surfaces denote negative spin densities. We were unable obtain a minimum structure for **4tBu-TIPS-Bz**. However, by replacing the TIPS group with a TMS group, minimum structures were found for both the singlet and triplet states. Comparative computations of **TMS-Bz** showed that this substitution change at the silyl unit has a small influence on the obtained triplet energy (0.01 eV difference).[7] Based on this result, the triplet energy of **4tBu-TMS-Bz** was used to extrapolate the triplet energy of **4tBu-TIPS-Bz,** yielding 3.02 eV.

Table S1: Computed triplet state energies of TIPS-ethynyl- and TMS-ethynyl-substituted benzenes.

Compound	E_T(DFT)[a] / eV	E_T(lit.)[b] / eV	E_T(DFT,corrected)[c] / eV
Benzene (Bz)	3.83	3.9	
TIPS-Bz	3.01		3.06
TMS-Bz	3.02		3.07
4tBu-TIPS-Bz	n.a.		3.02[d]
4tBu-TMS-Bz	2.98		3.03

[a] DFT-calculated triplet energy at the B3LYP/6-311+G(d,p) level of theory. [b] Experimental triplet energy from Ref[11]. [c] Calculated triplet energy corrected by the underestimation factor from benzene. [d] Estimated value from comparison of TIPS and TMS derivatives.

4. Additional spectroscopic measurements

4.1 Triplet state lifetime of TIPS-Bz

The triplet lifetime of **TIPS-Bz**, which combines the TTA decay constant (k_{TTA}) and the natural triplet lifetime, was measured for a solution of 25 µM **Ir** and 2 mM **TIPS-Bz** in Ar-saturated benzene after 355 nm laser pulses. The triplet lifetime of any given annihilator will strongly depend on the excitation intensity as k_{TTA} depends on the triplet state concentration.[12] For these selected conditions a monoexponential fit yielded a lifetime of 34 µs.

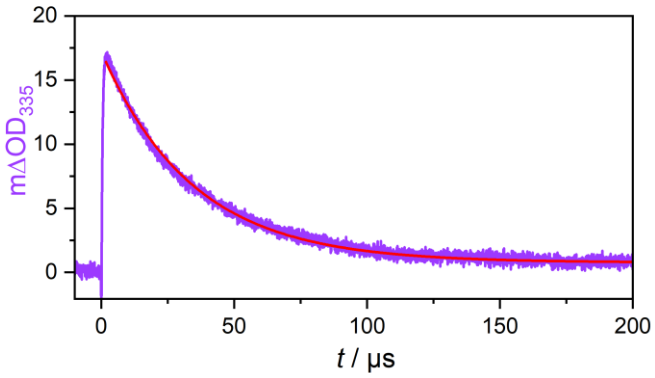

Figure S1: Kinetic TA measurements of a solution of 25 µM **Ir** and 2 mM **TIPS-Bz** in Ar-saturated benzene after 355 nm laser pulse excitation.

4.2 Control experiments

A common loss pathway in TTA-UC is the formation of singlet excimers, which leads to a reduction in emission energy. However, the irradiation of **TIPS-Bz** at 280 nm across a wide concentration range (80 µM to 16 mM) yielded identical emission spectra (Figure S2), indicating no detectable excimer formation.

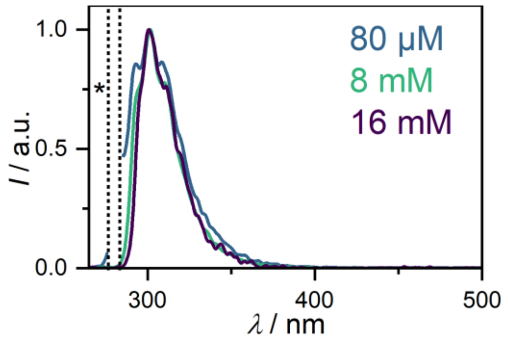

Figure S2: Emission spectrum of **TIPS-Bz** in Ar-saturated benzene after excitation at 280 nm with varying concentrations. Shorter wavelengths could not be used for excitation owing to the solvent absorption. The region around 280 nm (indicated with *) was removed owing to stray light artifacts.

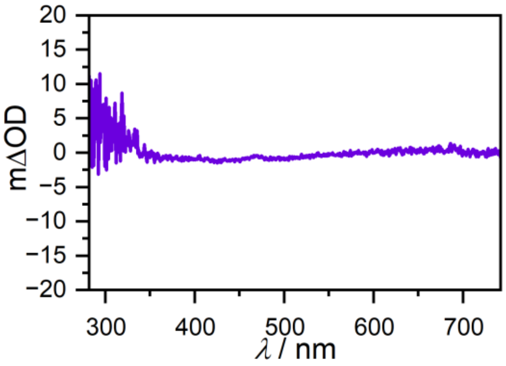

Figure S3: TA spectrum of 25 µM **Ir** and 2 mM **TIPS-Bz** recorded 130 µs after 355 nm laser excitation.

4.3 Photophysical properties of benzene and the TIPS-ethynyl substituted benzenes

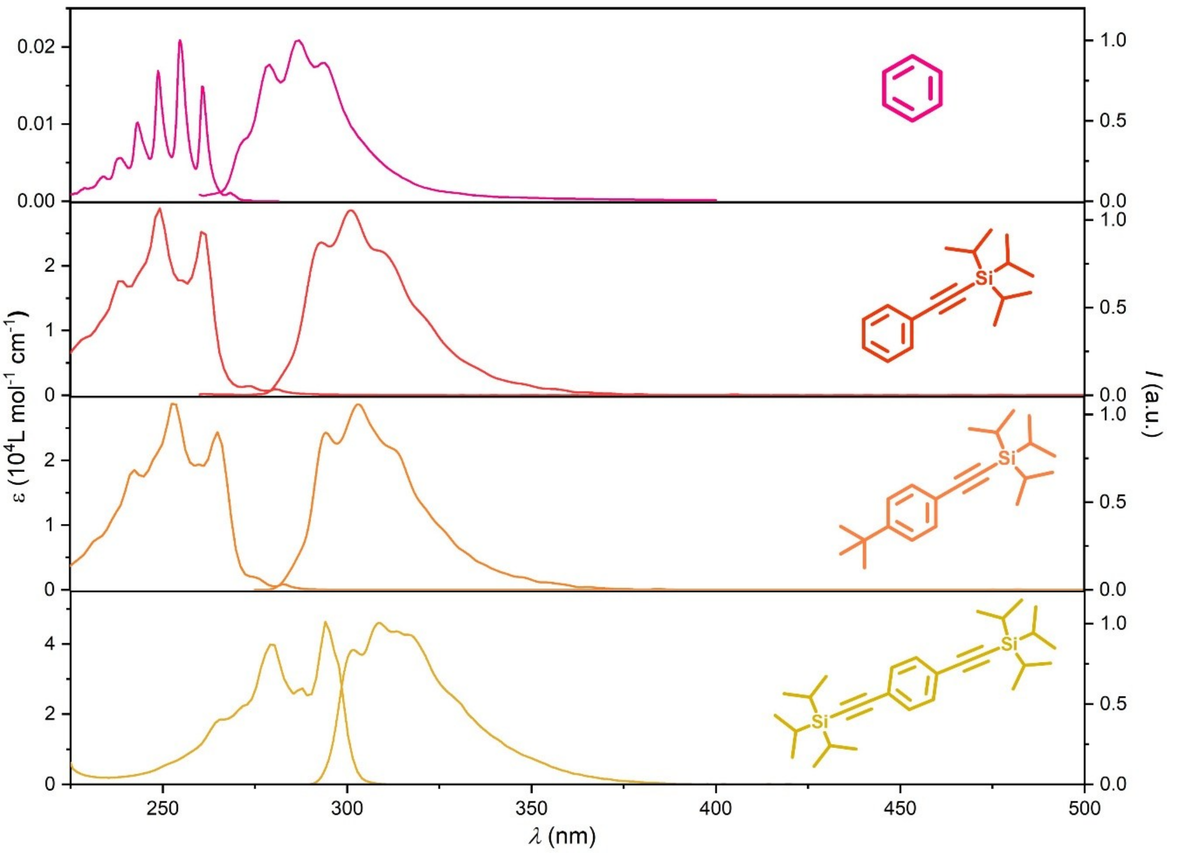

Figure S4: Molar absorption coefficients and emission spectra of benzene (taken from Ref[13]), **TIPS-Bz**, **4tBu-TIPS-Bz** and bTIPS-Bz (taken from Ref[7]) in cyclohexane.

Figure S4 presents the absorption and emission spectra of benzene and the corresponding annihilator structures. Substituting benzene with a TIPS-ethynyl group leads to a pronounced red shift in both spectra (compare Bz, **TIPS-Bz**, and bTIPS-Bz). In contrast, introducing a tert-butyl group at the para position relative to the TIPS-ethynyl group results in only a slight shift in the absorption and emission spectra (compare **TIPS-Bz** and **4tBu-TIPS-Bz**).

Table S2: Key photophysical properties of benzene and derived annihilator structures.

Compound	E_S / eV	Φ_Fl	τ_Fl / ns	E_T / eV
Benzene	4.76[a]	0.07[b]	34[a]	3.90[c]
TIPS-Bz	4.33	0.19[d]	19.9[d]	3.06[e]
4tBu-TIPS-Bz	4.31	–	14.7[d]	3.02[e]
bTIPS-Bz	4.14[d],[f]	0.48[d],[f]	2.8[d],[f]	2.64[f],[g]

[a] Taken from Ref[3]. [b] Taken from Ref[14,15]. [c] Taken from Ref[11]. [d] Measured in cyclohexane. [e] Obtained by DFT calculations (see Chapter S3). [f] Taken from Ref[7]. [g] Estimated from low temperature emission. DFT-calculated energy: 2.57 eV.

The key photophysical properties determined in this study, along with literature-reported values for these compounds, are summarized in Table S2. In general, increasing the number of TIPS-ethynyl groups lowers the singlet and triplet state energies as well as the fluorescence lifetime, while enhancing the fluorescence quantum yield. Substitution with a tert-butyl group in the para position further reduces the fluorescence lifetime (Figure S5), whereas its effect on the singlet state energy is minimal.

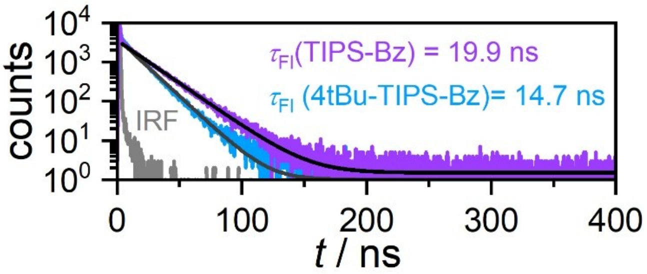

Figure S5: Fluorescence lifetime measurements of **TIPS-Bz** (purple) and **4tBu-TIPS-Bz** (blue) in cyclohexane, which had to be used instead of benzene to avoid solvent-derived background signals.

4.4 Optical power dependent UC measurements of the TIPS-Bz–Ir UC system

The upconversion intensity of the **TIPS-Bz–Ir** system was measured across a range of laser pulse energies (see main text and Figure 4C). The laser intensity was estimated as an optical power density, assuming a pulse duration of approximately 5 ns and an irradiated cuvette area of A = 1.4 cm^2 (see Equation 2). As an example, the optical power density was calculated for a pulse energy of 5.36 mJ:

$$P \approx \frac{Pulse\ energy}{t \times A} = \frac{5.36\ \mathrm{mJ}}{5\ \mathrm{ns} \times 1.4\ \mathrm{cm}^{-2}} = \ 766\ \mathrm{kW\ cm}^{-2} \quad (2)$$

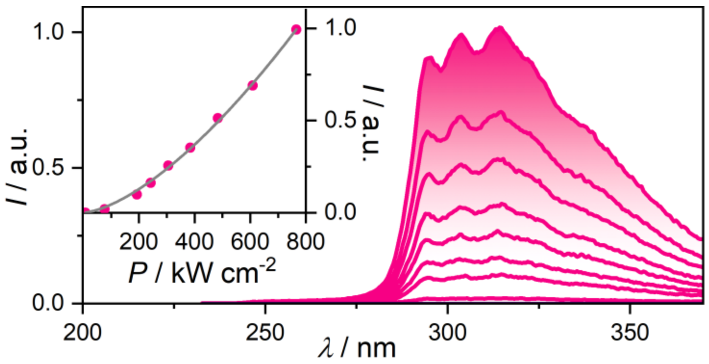

Figure S6: UC emission of 25 µM **Ir** and 2 mM **TIPS-Bz** in Ar-saturated benzene with 355 nm laser pulses with varying intensity. Inset: UC emission plotted against the laser energy recalculated as optical power density.

4.5 Estimation of UC quantum yield of the TIPS-Bz–Ir system

The UC quantum yield (ϕ_{UC}) of the **TIPS-Bz–Ir** system was estimated by comparing the quenched **Ir** emission with the UC emission following 355 nm laser excitation at 23.84 mJ. It was assumed that the emission quantum yield of **Ir** (ϕ_{Ir}), reported as 0.84 in THF, does not differ significantly in benzene.[1] Emission spectra were recorded from a solution containing 25 µM **Ir** and 2 mM **TIPS-Bz** in Ar-saturated benzene, under identical conditions but using different integration time windows. To prevent detector oversaturation, a grey filter (OD 2.0) was employed for integrating the quenched **Ir** emission (I_{quenched}) within the 0–4 µs window post-excitation, which was then compared to the UC emission integrated from 4–204 µs. The quenching efficiency η was determined to be 0.90.

$$\phi_{\mathrm{UC}} \approx \frac{I_{\mathrm{UC}} \times (1-\eta)}{I_{\mathrm{quenched}}} \times \phi_{\mathrm{Ir}} = 0.13\ \%$$

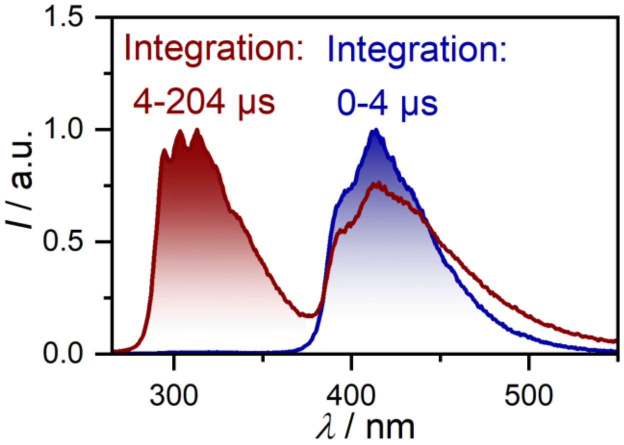

Figure S7: Time-gated emission spectra of 25 µM **Ir** and 2 mM **TIPS-Bz** in Ar-saturated benzene after 355 nm laser pulses.

5. Spectroscopic characterization of the 4tBu-TIPS-Bz–Ir UC system

The compound **4tBu-TIPS-Bz** was characterized as a potential annihilator analogous to **TIPS-Bz** in the main paper. Stern–Volmer quenching studies of **Ir** with **4tBu-TIPS-Bz** in Ar-saturated benzene with 355 nm laser pulses revealed a TTET constant of 3.26 10^{8} M^{-1} s^{-1} (Figure S8A). Even though DFT calculations suggested a decreased triplet energy of 3.02 eV with respect to **TIPS-Bz** the TTET constant is significantly lower. The additional sterically demanding group might hamper the required orbital overlap between energy donor and acceptor. The triplet-triplet absorption spectrum for **4tBu-TIPS-Bz** was recorded after complete deactivation of **Ir** (Figure S8B). A concentration of 6.25 µM **Ir** and 1mM **4tBu-TIPS-Bz** was used to minimize filter effects. The spectrum is slightly red-shifted compared to **TIPS-Bz** with a maximum absorption at 314 nm (main paper, Figure 3A). Further experiments were performed with concentration of 25 µM **Ir** and 2 mM **4tBu-TIPS-Bz**. Kinetic traces of ^{3}**4tBu-TIPS-Bz** and 25 µM **Ir** emission were recorded (Figure S8C), displaying concurrent formation and deactivation, respectively. Under the chosen conditions ^{3}**4tBu-TIPS-Bz** has an estimated lifetime of 38 µs, which is displayed in Figure S8D (monoexponentially fitted). A time-gated emission spectrum (integrated 10-210 µs after excitation) shows TTA-UC emission of **4tBu-TIPS-Bz**. However, apart from the sensitizer emission another signal in the UV is also detected that indicates degradation of the UC system. In conclusion, the UC performance of **4tBu-TIPS-Bz** does not benefit from the reduced triplet state energy with respect to **TIPS-Bz**.

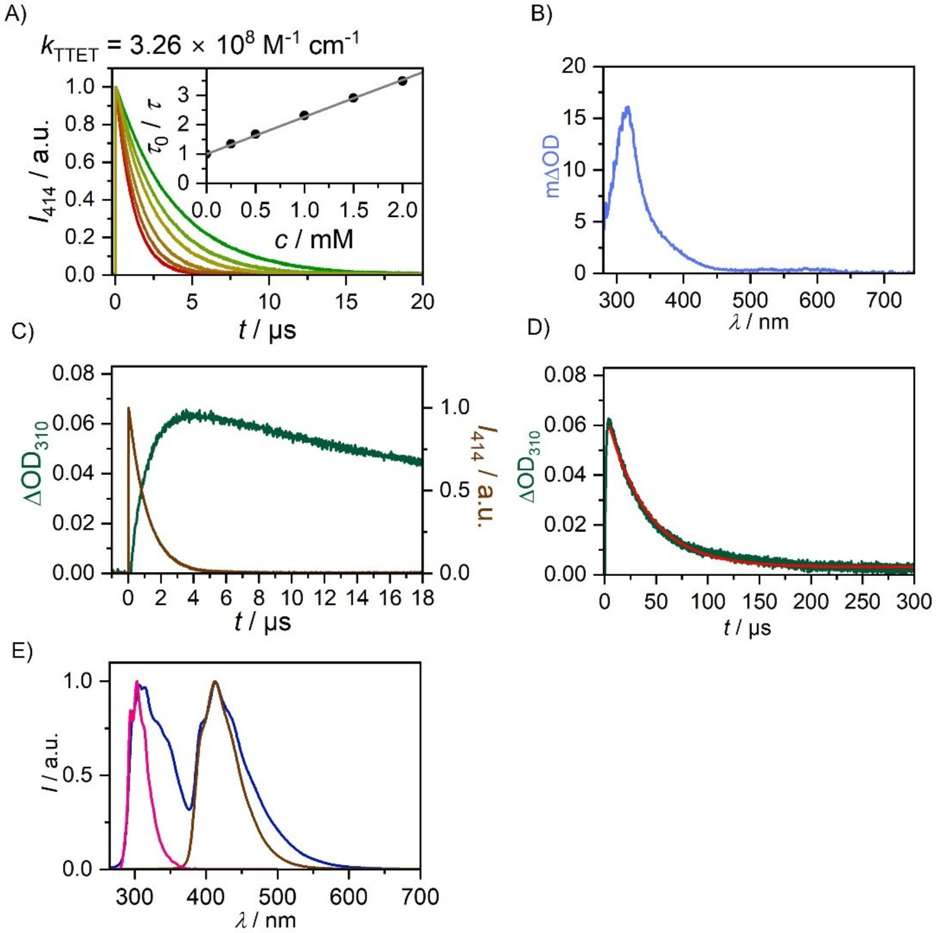

Figure S8: Mechanistic investigations of an Ar-saturated solution of **Ir** and **4tBu-TIPS-Bz** in benzene with 355 nm laser pulses. A) Stern-Volmer analysis with 25 µM **Ir** and varying concentrations of **4tBu-TIPS-Bz**. B) TA spectrum recorded 15 µs after excitation of 6.25 µM **Ir** and 1 mM **4tBu-TIPS-Bz**. C) and D) Kinetic traces of the transient ^{3}**4tBu-TIPS-Bz** and emission of ^{3}**Ir** of 25 µM **Ir** and 2 mM **4tBu-TIPS-Bz**. E) Time-gated emission spectrum of 25 µM **Ir** and 2 mM **4tBu-TIPS-Bz** recorded 10-210 µs after excitation (blue graph), in comparison to the emission of **4tBu-TIPS-Bz** (pink) and **Ir** (brown) after direct excitation at 280 nm.

5.1 Photostability measurements of TIPS-Bz–Ir and 4tBu-TIPS-Bz–Ir

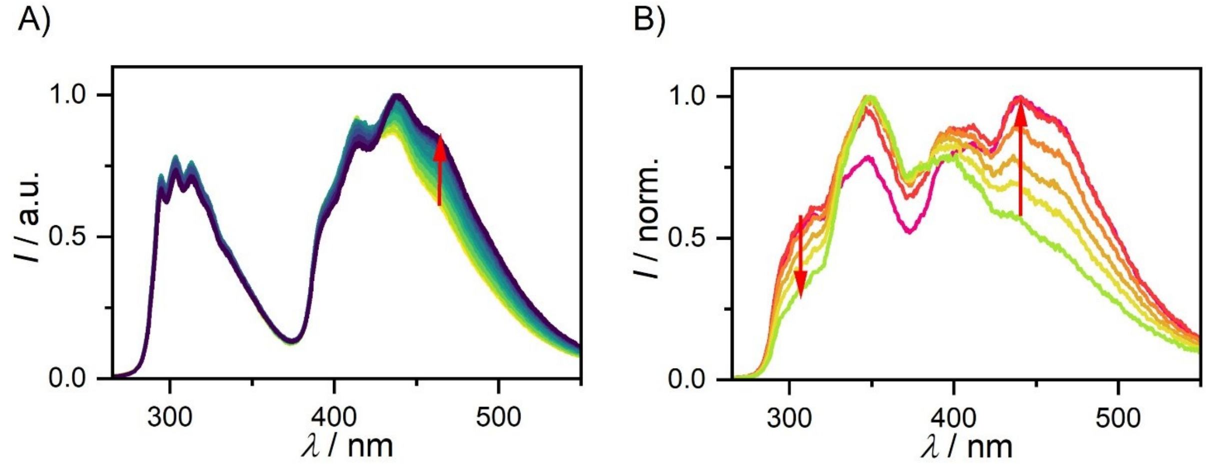

Figure S9: Photostability measurements of **TIPS-Bz**–**Ir** and **4tBu-TIPS-Bz**–**Ir** UC systems under 355 nm laser pulses (~20 mJ). A) UC emission of 25 µM **Ir** and 2 mM **TIPS-Bz** in Ar-saturated benzene after individual 355 nm laser pulses (first pulse, yellow; last pulse, dark blue; 100 pulses in total). B) UC emission of 25 µM **Ir** and 2 mM **4tBu-TIPS-Bz** in Ar-saturated benzene over 20 averaged 355 nm laser pulses.

The photostability of the UC systems **TIPS-Bz–Ir** and **4tBu-TIPS-Bz–Ir** under 355 nm laser irradiation was investigated. **TIPS-Bz–Ir** exhibited significantly greater stability, with only minor spectral changes indicating limited degradation (Figure S9A). Moreover, its UC emission intensity remained largely constant over 100 laser pulses. In contrast, the **4tBu-TIPS-Bz–Ir** system showed pronounced degradation, evidenced by strong emission signals likely originating from degradation products (Figure S9B).

6. NMR and FD mass spectra

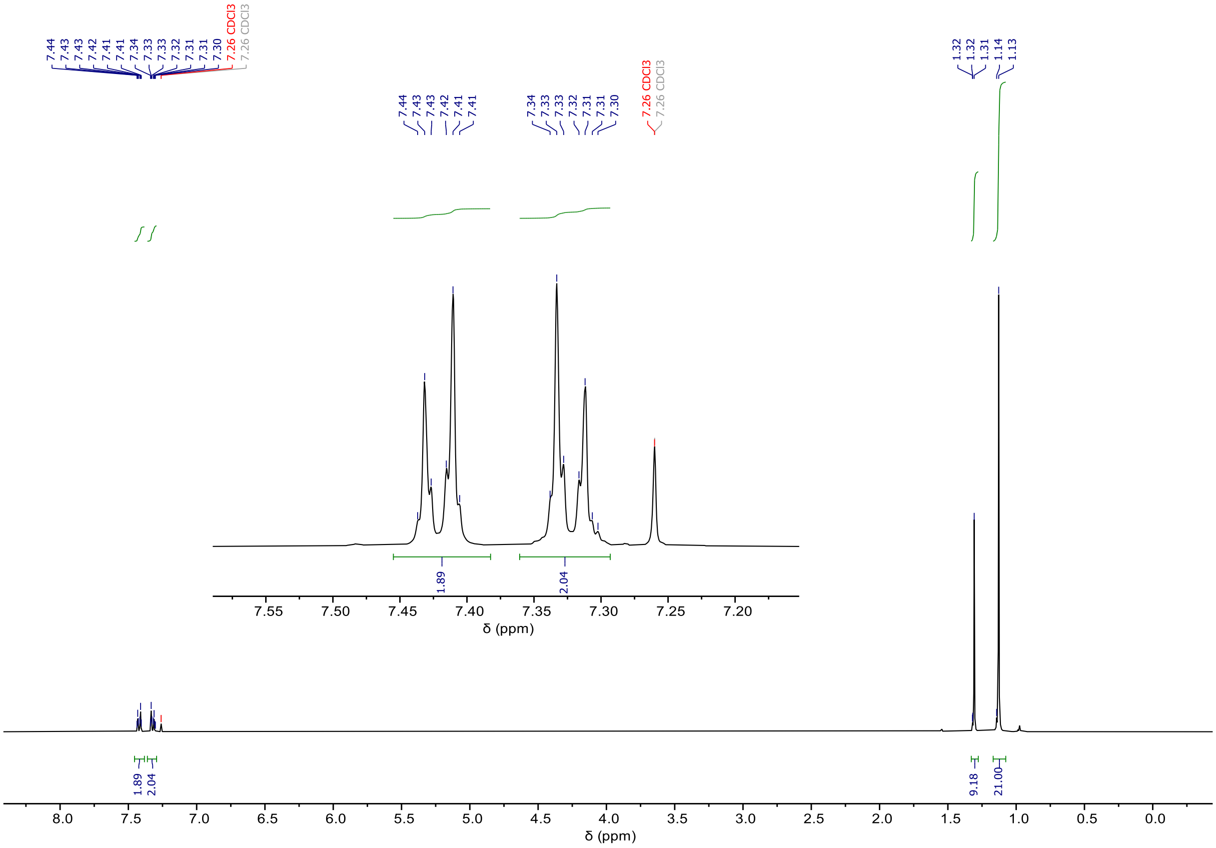

Figure S10: ^{1}H NMR spectrum of **4tBu-TIPS-Bz** in CDCl$_3$.

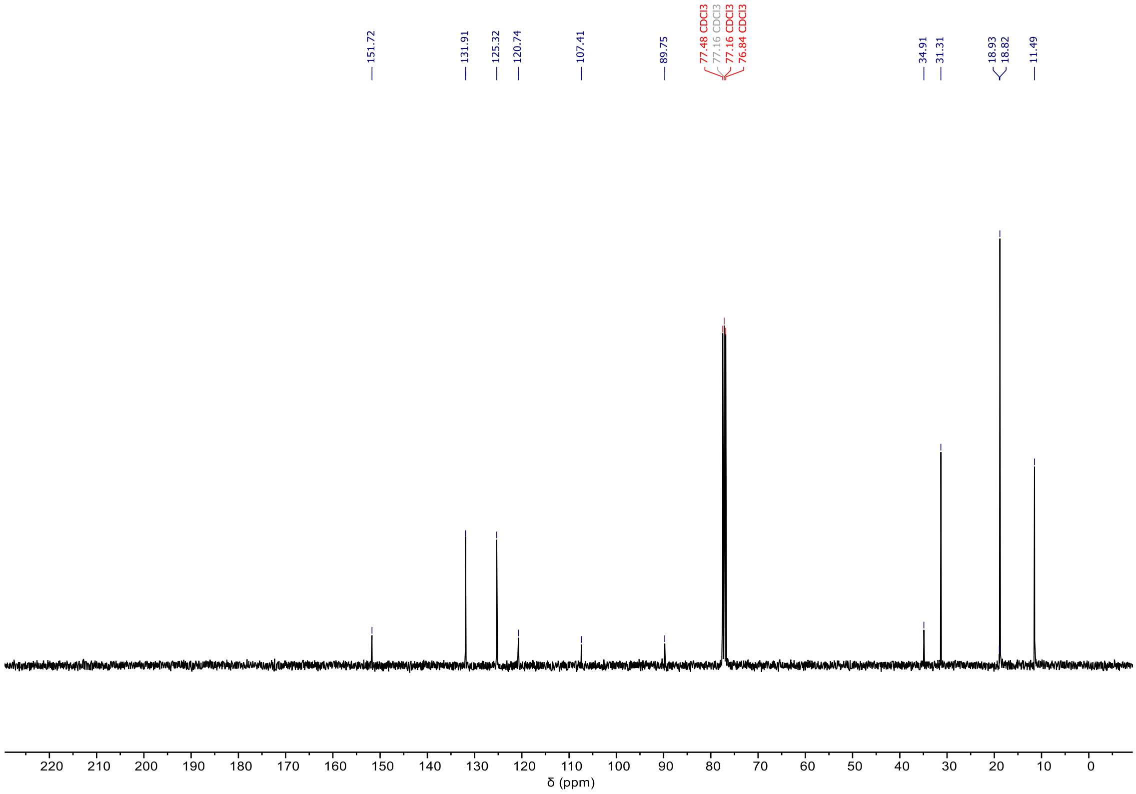

Figure S11: ^{13}C NMR spectrum of **4tBu-TIPS-Bz** in CDCl$_3$.

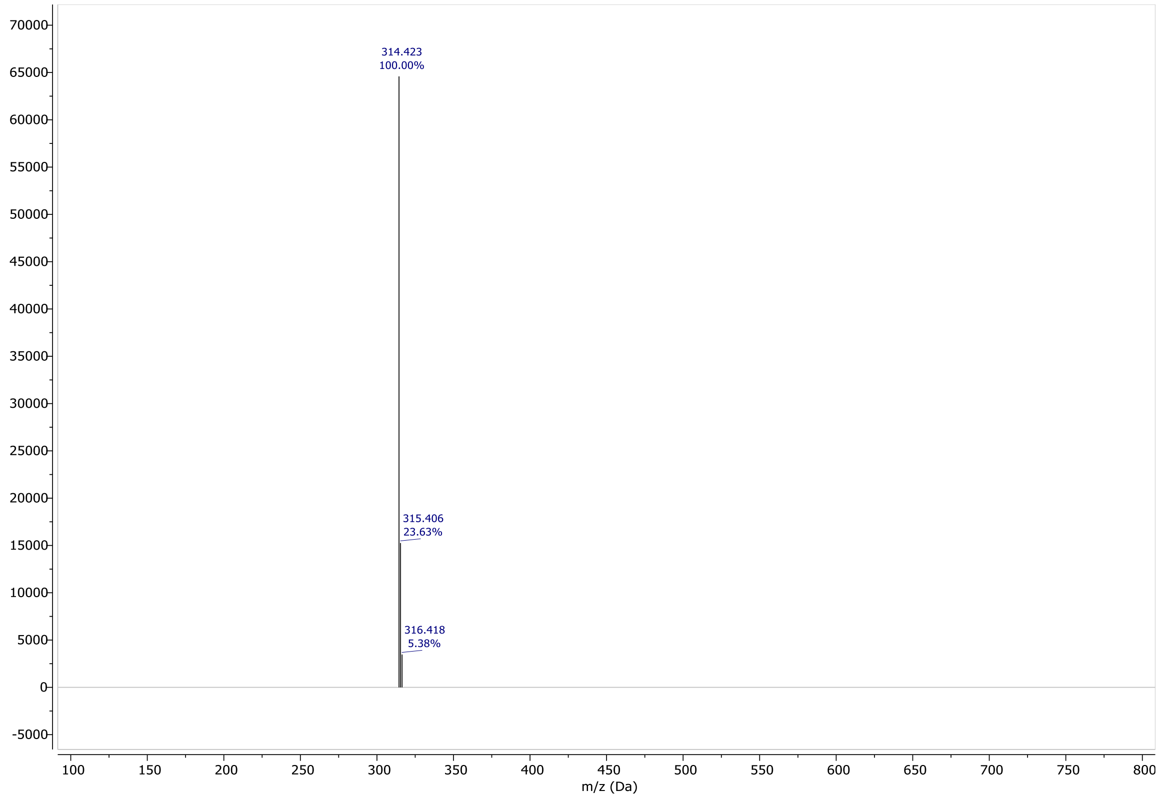

Figure S12: FD mass spectrum of **4tBu-TIPS-Bz**.

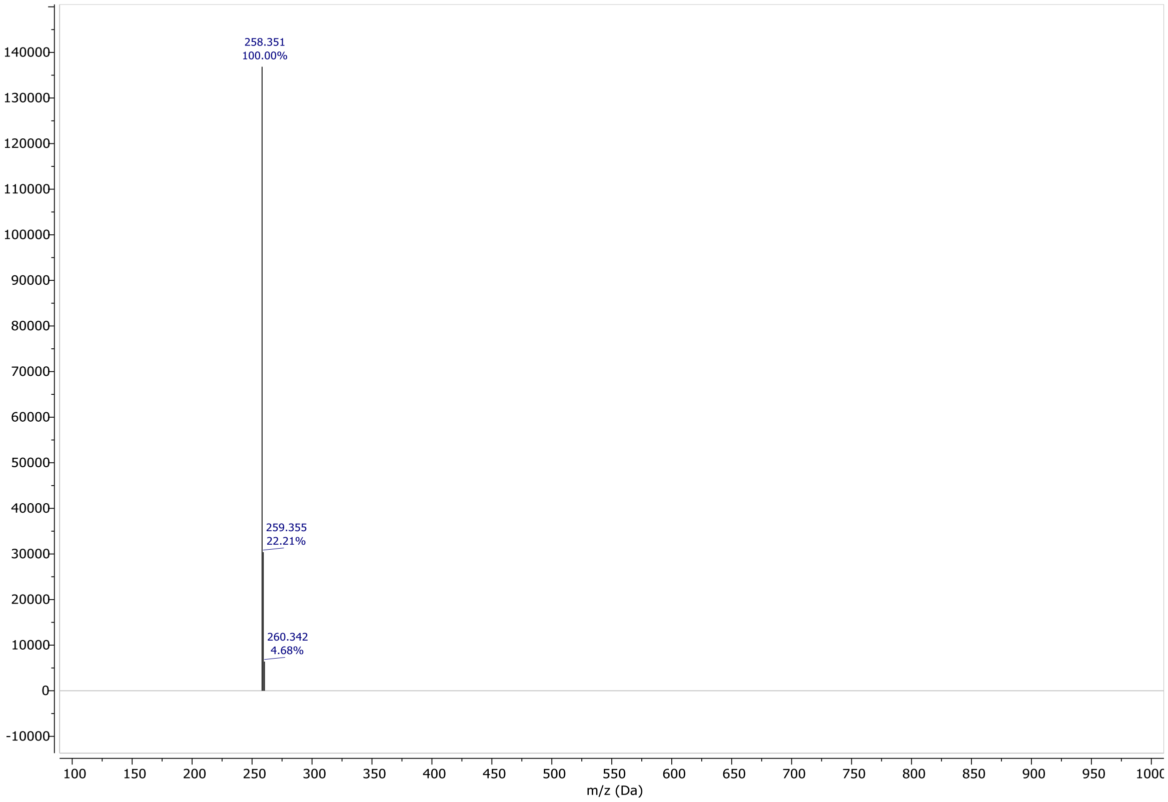

Figure S13: FD mass spectrum of **TIPS-Bz**.

7. References

1. K. Tsuchiya, S. Yagai, A. Kitamura, T. Karatsu, K. Endo, J. Mizukami, S. Akiyama and M. Yabe, *Eur. J. Inorg. Chem.*, 2010, **2010**, 926–933.
2. T. O. Paulisch, L. A. Mai, F. Strieth-Kalthoff, M. J. James, C. Henkel, D. M. Guldi and F. Glorius, *Angew. Chem. Int. Ed.*, 2022, **61**, e202112695.
3. M. Montalti, A. Credi, L. Prodi and M. T. Gandolfi, *Handbook of Photochemistry*, CRC Press, 0 edn., 2006.
4. H. E. Gottlieb, V. Kotlyar and A. Nudelman, *J. Org. Chem.*, 1997, **62**, 7512–7515.
5. N. Harada, Y. Sasaki, M. Hosoyamada, N. Kimizuka and N. Yanai, *Angew. Chem. Int. Ed.*, 2021, **60**, 142–147.
6. T. J. B. Zähringer, M.-S. Bertrams and C. Kerzig, *J. Mater. Chem. C*, 2022, **10**, 4568–4573.
7. T. J. B. Zähringer, J. A. Moghtader, M. Bertrams, B. Roy, M. Uji, N. Yanai and C. Kerzig, *Angew. Chem. Int. Ed.*, 2023, **62**, e202215340.
8. Q. Chen, L. Fu, J. You and Y. Nishihara, *Synlett*, 2021, **32**, 1560–1564.
9. F. Neese, *WIREs Comput. Mol. Sci.*, 2012, **2**, 73–78.
10. M. D. Hanwell, D. E. Curtis, D. C. Lonie, T. Vandermeersch, E. Zurek and G. R. Hutchison, *J. Cheminformatics*, 2012, **4**, 17.
11. J. P. Doering, *J. Chem. Phys.*, 1969, **51**, 2866–2870.
12. Y. Murakami and K. Kamada, *Phys. Chem. Chem. Phys.*, 2021, **23**, 18268–18282.
13. I. B. Berlman, *Handbook of fluorescence spectra of aromatic molecules*, Academic Press, New York, 2d ed., 1971.
14. W. R. Dawson and M. W. Windsor, *J. Phys. Chem.*, 1968, **72**, 3251–3260.
15. M. Luria, M. Ofran and G. Stein, *J. Phys. Chem.*, 1974, **78**, 1904–1909.